

Synthetic-to-Real Camouflaged Object Detection

Zhihao Luo

Fuzhou University

Fuzhou, China

zhluo2003@gmail.com

Luojun Lin*

Fuzhou University

Fuzhou, China

linluojun2009@126.com

Zheng Lin*

Tsinghua University

Beijing, China

frazer.linzheng@gmail.com

Abstract

Due to the high cost of collection and labeling, there are relatively few datasets for camouflaged object detection (COD). In particular, for certain specialized categories, the available image dataset is insufficiently populated. Synthetic datasets can be utilized to alleviate the problem of limited data to some extent. However, directly training with synthetic datasets compared to real datasets can lead to a degradation in model performance. To tackle this problem, in this work, we investigate a new task, namely Syn-to-Real Camouflaged Object Detection (S2R-COD). In order to improve the model performance in real world scenarios, a set of annotated synthetic camouflaged images and a limited number of unannotated real images must be utilized. We propose the Cycling Syn-to-Real Domain Adaptation Framework (CSRDA), a method based on the student-teacher model. Specially, CSRDA propagates class information from the labeled source domain to the unlabeled target domain through pseudo labeling combined with consistency regularization. Considering that narrowing the intra-domain gap can improve the quality of pseudo labeling, CSRDA utilizes a recurrent learning framework to build an evolving real domain for bridging the source and target domain. Extensive experiments demonstrate the effectiveness of our framework, mitigating the problem of limited data and handcraft annotations in COD. Our code is publicly available at <https://github.com/Muscape/S2R-COD>.

CCS Concepts

- Computing methodologies → Scene understanding; Image segmentation.

Keywords

Camouflaged Object Detection; Synthetic-to-Real; Noisy Label Learning

ACM Reference Format:

Zhihao Luo, Luojun Lin, and Zheng Lin. 2025. Synthetic-to-Real Camouflaged Object Detection. In *Proceedings of the 33rd ACM International Conference on Multimedia (MM '25), October 27–31, 2025, Dublin, Ireland*. ACM, New York, NY, USA, 10 pages. <https://doi.org/10.1145/3746027.3755461>

*L. Lin and Z. Lin are corresponding authors.

Permission to make digital or hard copies of all or part of this work for personal or classroom use is granted without fee provided that copies are not made or distributed for profit or commercial advantage and that copies bear this notice and the full citation on the first page. Copyrights for components of this work owned by others than the author(s) must be honored. Abstracting with credit is permitted. To copy otherwise, or republish, to post on servers or to redistribute to lists, requires prior specific permission and/or a fee. Request permissions from permissions@acm.org.

MM '25, Dublin, Ireland

© 2025 Copyright held by the owner/author(s). Publication rights licensed to ACM.

ACM ISBN 979-8-4007-2035-2/2025/10

<https://doi.org/10.1145/3746027.3755461>

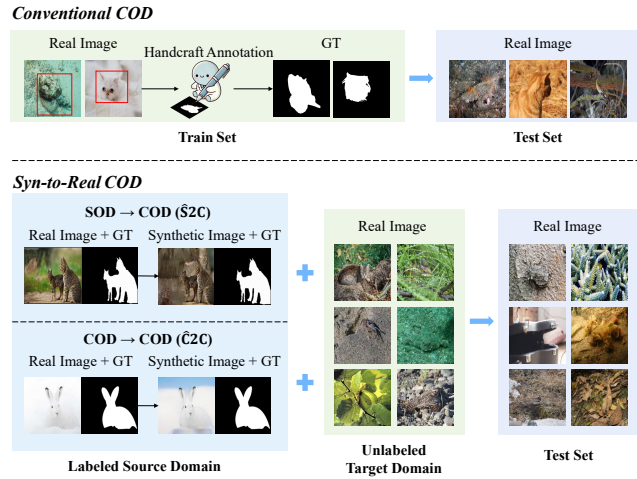


Figure 1: The difference between Conventional COD and Syn-to-Real COD. In conventional COD tasks, annotated data is scarce due to the difficulty of obtaining camouflaged objects, and handcraft annotation is costly, but Syn-to-Real COD approach utilizes synthetic data for supervised training and adapts to real, unlabeled images.

1 Introduction

Camouflaged object detection (COD) focuses on identifying objects that blend seamlessly into their surroundings, characterized by low contrast, blurred boundaries, and a high degree of similarity between the object and the background [18, 26, 60, 66, 67]. These features make COD significantly more challenging than standard object detection tasks. While substantial progress has been made in recent years [6, 31, 49, 70, 74], the complexity of real world scenes has rendered handcraft annotation both time-consuming and costly. For instance, annotating a single image in COD10K dataset takes approximately one hour [11], which limits the availability of datasets and restricts their diversity to a small range of species.

Data scarcity and the high cost of handcrafted annotation are common problems in many research areas. Using synthetic images to replace real data has become an effective and widely adopted strategy. In recent years, various methods for generating synthetic images have been proposed, such as LAKE-RED [72], a method was proposed to generate synthetic camouflaged object images, with the aim of addressing the scarcity of real datasets and the limited number of images for certain species. Although the generated data set partially alleviates these issues, directly training models on synthetic images often degrades performance. A comparison between synthetic and real images reveals significant shortcomings in the synthetic data. These images appear designed solely to achieve the

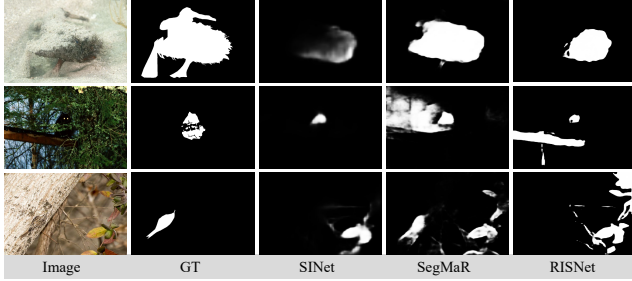


Figure 2: The output results of different models on the test set when trained using only source domain (synthetic images).

goal of blending objects into backgrounds, overlooking the realistic existence of objects. For example, as shown in Fig. 1, the rabbit appears to be placed against a sky background, and the cats look unnaturally embedded in the rock. These scenarios are highly improbable under real world conditions. Furthermore, as illustrated in Fig. 2, even the advanced model RISNet [58] performs poorly when trained solely on synthetic source domain images.

To address this limitation, we introduce the concept of Unsupervised Domain Adaptation (UDA). UDA is an effective approach to address the distribution shift between the source and target domain [3], particularly in scenarios where labeled data is scarce. In most applications, the training dataset is usually derived from the source domain, while the target domain is the scenario in which the model is actually applied. Therefore, we propose a novel task in this paper: Syn-to-Real Camouflaged Object Detection (S2R-COD). As shown in Fig. 1, we compare conventional COD with our proposed S2R-COD. Categorizing tasks into $\hat{S}2C$ and $\hat{C}2C$, $\hat{S}2C$ denotes using SOD dataset synthetic camouflaged dataset as the source domain. $\hat{C}2C$ indicates utilization of COD dataset as a synthetic camouflaged dataset for the source domain, noting that the source and target domain data do not overlap. The model is ultimately evaluated on the test set of real images. By effectively adapting from the synthetic domain to the real domain, this task provides a pathway to enhance the generalization capability of COD models, ultimately improving their performance in real world scenarios.

To effectively tackle the challenges posed by the S2R-COD task, we introduce a novel framework named Cycling Syn-to-Real Domain Adaptation Framework (CSRDA) that encourages pseudo labels generation and domain adaptation training to mutually benefit from a curriculum learning approach. The training process consists of two main stages: first, in inter-domain transfer phase, the student model is trained on the source domain data using supervised learning, while the target domain data is utilized in a consistency based unsupervised approach. To enhance adaptation, we introduce a customized Edge-Aware Saliency-Weighted Loss (ES Loss), which preserves edge structures and emphasizes salient regions by dynamically weighting pseudo labels. In this process, the teacher model is updated using the exponential moving average (EMA) [56] of the student model. Then, in intra-domain transfer phase, we fix the trained student and teacher models and use them to generate pseudo labels for the target domain. These pseudo labels are filtered based on Confident Label Selection (CLS) mechanism and then bridged with the source domain data to construct an evolving

real domain for the next training iteration. This process gradually reduces the domain gap and improves pseudo label quality.

We use SINet [11] as the baseline model and train it with the proposed method, which is further extended to several classic COD models, such as SINet-v2 [9], SegMaR [27], and RISNet [58]. We conducted extensive experiments on multiple datasets, including HKU-IS [38], CAMO [35], CHAMELEON [52], NC4K [44], and COD10K [11], evaluating the effectiveness of the proposed method. The results show that the model trained with our approach achieves significant performance improvements in the target domain while maintaining stable performance across different datasets, demonstrating its effectiveness and broad applicability.

Overall, our contributions are summarized as follows:

- We introduce the Syn-to-Real Camouflaged Object Detection (S2R-COD) task, establishing a new benchmark where synthetic data serves as the source domain and unlabeled real world data as the target domain.
- We provide extensive strong benchmarks for S2R-COD by systematically evaluating traditional domain adaptation methods on multiple classic COD models.
- We propose a Cycling Syn-to-Real Domain Adaptation Framework (CSRDA) based on student-teacher model. To boost domain adaptation, we design an Edge-Aware Saliency-Weighted Loss (ES Loss) and a Confident Label Selection (CLS) mechanism to align source and target domain progressively. Extensive experiments validate its effectiveness.

2 Related Works

2.1 Camouflaged Object Detection

Camouflaged Object Detection (COD) is a challenging computer vision task that focuses on identifying objects intentionally blended into their surroundings [29, 31, 37, 42, 47, 69]. The development of COD can be broadly divided into two stages: the traditional phase and the deep learning phase [40, 43, 59, 63, 65, 68, 75]. Traditional methods primarily used handcrafted features to differentiate camouflaged objects from their background, including texture [12], intensity [55], and color [50]. These features were used to compute attributes such as 3D convexity [48], optical flow [21], etc. These traditional methods perform well in simple scenarios but struggle with more complex cases. Deep learning has significantly advanced COD by enabling models to learn complex and high-level representations from data [20, 23, 41, 46, 53]. Existing deep learning based COD methods can be broadly categorized into CNN-based and Transformer-based approaches. a) CNN-based: SINet [11] uses the search and identification strategy to replicate the predation process of animals, achieving segmentation. SINet-v2 [9] proposes a neighbor connection decoder to refine feature representations, and group-reversal attention improves coarse predictions. DGNet [25] introduces the deep gradient network, which utilizes gradient-induced transitions to automatically group features. MFFN [73] employs Co-attention of multi-view to mine the complementary relationships and use the channel fusion module to conduct progressive context cue mining. b) Transformer-based: FSPNet [24] leverages nonlocal token enhancement for improved feature interaction and utilizes a feature shrinkage decoder to aggregate

camouflaged object cues better. RISNet [58] utilizes DepthGuided Feature Decoder merged RGB features and depth features, iterative feature refinement for improved small object detection. However, while these methods perform well on real images, their performance deteriorates on synthetic images. Therefore, we propose a new benchmark that combines domain adaptation from synthetic to real images with camouflaged object detection.

2.2 Unsupervised Domain Adaptation

The core idea of Unsupervised Domain Adaptation (UDA) is to improve performance on the target domain by learning from the source domain and narrowing the distributional gap between the source and target domain without requiring labeled data from the target domain. Among the various techniques developed for domain adaptation, three commonly explored approaches include divergence-based methods, adversarial learning, and image-to-image translation with style transfer. a) Divergence: MMD [15, 16] is a statistical test used to determine if two distributions are equivalent based on their samples. CAN [30] minimizes cross-entropy loss on labeled target data while alternating between estimating labels for target samples. b) Adversarial Learning: DANN [1, 13, 14] train the feature extractor by negating the gradient from the domain classifier using a gradient reversal layer during backpropagation. In ADDA [57], the feature extractor is trained by inverting the labels for the domain classifier, making it learn domain-invariant representations. Shen et al. [51] proposed WDGR by modifying DANN, replacing the domain classifier with a network that directly approximates the Wasserstein distance. Recently, teacher-student paradigms [56] such as PMT [2] have been explored to enhance target representation learning through soft supervision and class-level alignment. C) Image-to-Image Translation and Style Transfer: CycleGAN [77], based on pix2pix, is a commonly used unsupervised image-to-image translation method, along with similar approaches like DualGAN [64] and DiscoGAN [32]. FDA [62] uses Fast Fourier Transform to propose a simple method for domain alignment that does not require any learning. In addition to these classical techniques, recent efforts have started leveraging large-scale pre-trained vision-language models to improve cross-domain generalization [34]. Unlike the aforementioned methods, our approach explicitly frames UDA as a robust and efficient noisy label learning task, simplifying the challenge and delivering enhanced performance.

3 Method

3.1 Problem Setup

From the perspective of unsupervised domain adaptation, we propose the first baseline model for S2R-COD. Given two domains, source domain \mathcal{D}_s by generating models g from auxiliary real datasets \mathcal{D}_r synthesized to obtain:

$$(x_s, y_s) = g(x_r, y_r), \quad g \in \mathcal{G}_{COD-GEN}, \quad (1)$$

where $(x_s, y_s) \in \mathcal{D}_s$, and $(x_r, y_r) \in \mathcal{D}_r$, x_s and x_r denote source and origin real images, respectively, y_s, y_r are their corresponding ground truths. $\mathcal{G}_{COD-GEN}$ is a method for generating synthetic COD images, such as LAKE-RED [72], which embeds the ground truth y_r in a random camouflaged background through a generative technique. The target domain \mathcal{D}_t consists of unlabeled real

camouflaged images. Note that \mathcal{D}_t is distinct from \mathcal{D}_r in terms of real images.

$$P(\mathcal{D}_t) \neq P(\mathcal{D}_r), \quad (2)$$

where P denotes the data distribution. Our goal is to train a model $f : \mathcal{X} \rightarrow \mathcal{Y}$ using the domain adaptation method to use only the labeled data \mathcal{D}_s and the unlabeled data \mathcal{D}_t , aiming to optimize the following objective:

$$\min_f \mathbb{E}_{(x_s, y_s) \sim \mathcal{D}_s, x_t \sim \mathcal{D}_t} [\mathcal{L}(f(x_s, x_t)), y_s], \quad (3)$$

where \mathcal{L} is total loss function and y_t is unknown and inaccessible. The entire learning process is shown in Fig. 3.

3.2 Stage A: Inter-Domain Transfer

We employ an EMA model f_{ema} to generate pseudo labels inspired by the Mean Teacher [56], which has been widely used in self-supervised and semi-supervised learning [17]. By leveraging temporal ensembling, EMA produces more reliable pseudo labels, improving their quality. In our framework, the teacher model f_{ema} and the student model f share the same backbone network (e.g., SINet [11]) but take different image views as input, teacher model takes the weakly augmented image $\mathcal{A}(x_t)$, student model uses the weakly augmented image $\mathcal{A}(x_s)$ in the source domain and the strongly augmented image $\tilde{\mathcal{A}}(x_t)$ in the target domain. During different training iterations, the teacher model is updated using the EMA of the student model. The weight of the teacher model can be expressed as follows:

$$f_{ema} = \lambda f_{ema} + (1 - \lambda) f, \quad (4)$$

where λ is the smoothing coefficient that controls the update momentum of teacher model. The optimization goal is defined as:

$$\begin{aligned} \min_f \mathbb{E}_{(x_s, y_s) \sim \mathcal{D}_s, x_t \sim \mathcal{D}_t} [\mathcal{L}_{CE}(f(\mathcal{A}(x_s)), y_s)] \\ + [\mathcal{L}_{ES}(f(\tilde{\mathcal{A}}(x_t)), f_{ema}(\mathcal{A}(x_t)))], \end{aligned} \quad (5)$$

where \mathcal{L}_{CE} is fully supervised loss of the student model using binary cross-entropy loss on source domain, and \mathcal{L}_{ES} is customized loss function between the student model and teacher model.

Edge-Aware Saliency-Weighted Loss. To enhance the model ability to preserve edge structures and improve the learning of salient regions in cross domain camouflaged object detection, we designed an Edge-Aware Saliency-Weighted loss. This loss consists of two parts, the edge alignment loss and the significant region weighting loss. The total loss is formulated as:

$$\mathcal{L}_{ES} = \alpha \mathcal{L}_{EA} + \beta \mathcal{L}_{SW}, \quad (6)$$

where α and β are hyperparameters that balance the contributions of edge alignment and saliency weighted losses. Edge alignment loss is defined as follows:

$$\mathcal{L}_{EA} = \mathbb{E}_{x_t \sim \mathcal{D}_t} \|\nabla f(\tilde{\mathcal{A}}(x_t)) - \nabla f_{ema}(\mathcal{A}(x_t))\|_1, \quad (7)$$

where ∇ represents the sobel edge operator, which is used to extract the edge intensity maps of the outputs from both the student and teacher models. The alignment of the edge structure between the two models is then enforced using the loss of L1. To strengthen the student model focus on salient regions, dynamic weights are

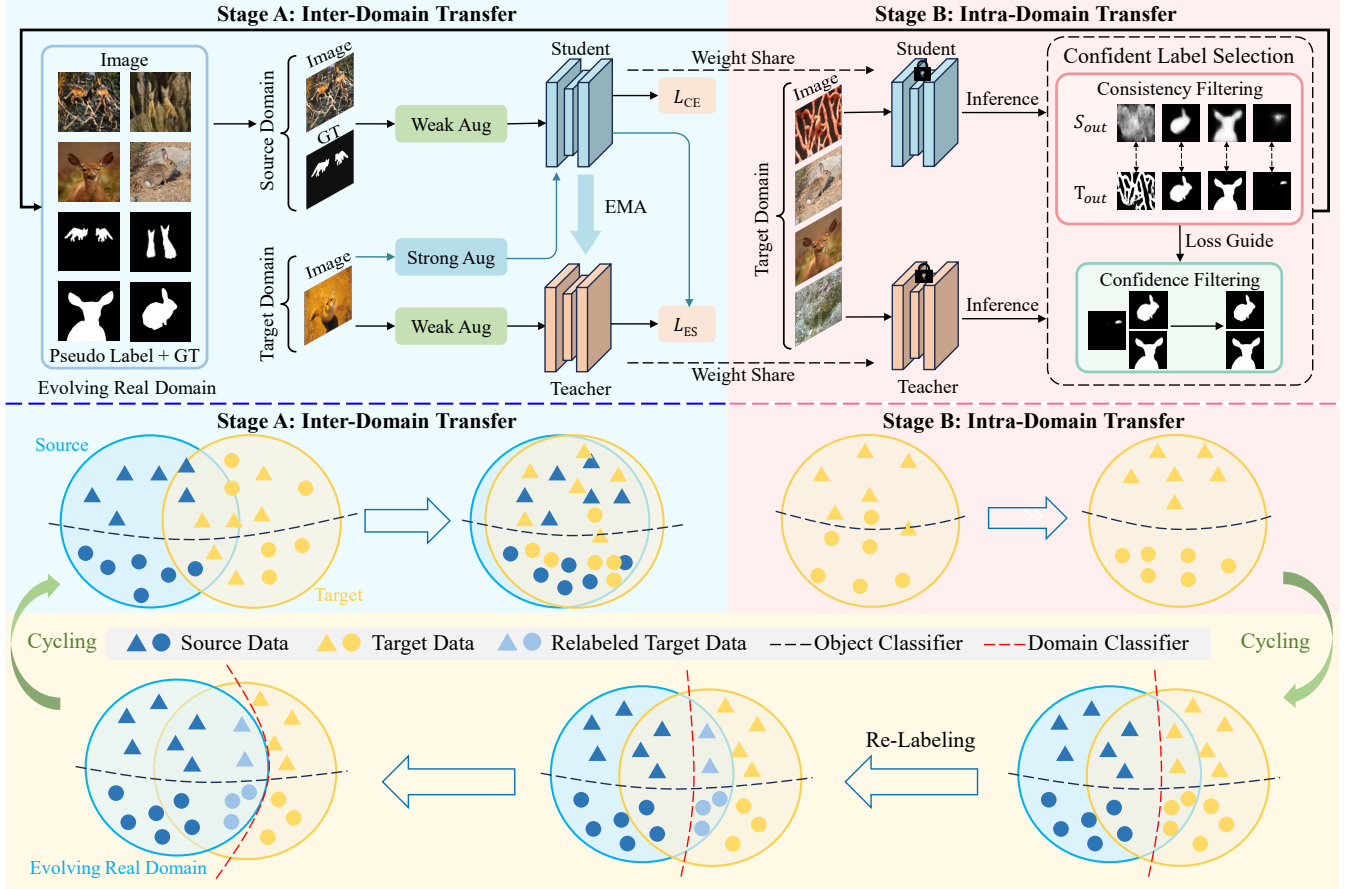


Figure 3: The overall pipeline of our CSRDA. 1) Stage A: EMA [56] based student-teacher co-training with augmented synthetic source and real target data. 2) Stage B: Confident Label Selection (CLS) evaluates the reliability of pseudo labels, and high confidence target domain samples are relabeled as source domain samples. Evolving Real Domain mechanism bridges domain gaps through a progressive domain alignment strategy, optimizing the cross domain feature space.

assigned to the pseudo labels \hat{y}_t generated by the teacher model, and weighted cross-entropy is calculated:

$$\mathcal{L}_{SW} = \mathbb{E}_{x_t \sim \mathcal{D}_t} \{ W [\hat{y}_t \log f(\tilde{\mathcal{A}}(x_t)) + (1 - \hat{y}_t) \log (1 - f(\tilde{\mathcal{A}}(x_t)))] \}. \quad (8)$$

The weight vector $W = \hat{y}_t + \delta$, where δ is a hyperparameter that boosts the weight of \mathcal{L}_{SW} . By reducing the weight of background or noise regions and increasing the weight of the prominent target regions, the interference of noise signals is mitigated while enhancing the model ability to fit key regions.

3.3 Stage B: Intra-Domain Transfer

In the field of unsupervised image segmentation, the integration of noisy labels has emerged as a significant challenge. Since the generated noisy labels contain task related information cues, they can impose task specific regularization on the optimization process of unsupervised image segmentation. Inspired by the small-loss selection strategy in noisy label learning [28], we propose a Confident Label Selection (CLS) mechanism to filter the pseudo labels

generated by the teacher model in the target domain, extracting the cleaner portions and removing samples with high noise. Thus, we construct a high confidence pseudo label subset $\mathcal{D}_{cl} \subseteq \mathcal{D}_t$ to reduce the impact of low quality pseudo labels on model training. Specifically, we leverage the prediction consistency between the teacher and student models in the target domain to assess the reliability of the pseudo labels and construct a high confidence pseudo label set based on the following criteria:

$$\mathcal{D}_{cl} = \{ (x_t^{cl}, y_t^{cl}) \mid \mathcal{L}_{ES}(f(x_t^{cl}), f_{ema}(x_t^{cl})) \leq \mu \mathbb{E}_{x_t \sim \mathcal{D}_t} \mathcal{L}_{ES}(f(x_t), f_{ema}(x_t)) \}, \quad (9)$$

where $x_t^{cl} \in \mathcal{D}_t$ and $y_t^{cl} = f_{ema}(x_t^{cl})$, μ is a hyperparameter controls the selection ratio of pseudo labels, and the student and teacher models have fixed weights during this process. By dynamically selecting \mathcal{D}_{cl} using the threshold μ , an adaptive learning strategy [36] is essentially constructed. Furthermore, we impose a confidence constraint on the filtered pseudo labels, setting regions with a confidence lower than the threshold τ to zero and removing samples with overall confidence below τ , ensuring that the model primarily

Table 1: Experimental results on HKU-IS → COD10K ($\hat{S}2C$) benchmark. \uparrow indicates the higher the score the better, and \downarrow indicates the lower the better. The best results are marked in bold. The same representation is in the following tables.

Model	Setting	$S_\alpha \uparrow$	$F_\beta^w \uparrow$	$E_\phi^{ad} \uparrow$	$E_\phi^{mn} \uparrow$	$E_\phi^{mx} \uparrow$	$F_\beta^{ad} \uparrow$	$F_\beta^{mn} \uparrow$	$F_\beta^{mx} \uparrow$	$M \downarrow$
SINet [11]	Source-Only	0.6418	0.3707	0.7323	0.6570	0.7211	0.4653	0.4284	0.4718	0.0905
	Mean Teacher	0.6984	0.4165	0.7092	0.7177	0.7805	0.4888	0.5106	0.5598	0.0915
	Ours	0.7136	0.4814	0.7676	0.7443	0.7950	0.5548	0.5572	0.5960	0.0717
SINet-v2 [9]	Source-Only	0.6466	0.4121	0.7332	0.6986	0.7035	0.4736	0.4640	0.4697	0.0976
	Mean Teacher	0.6485	0.4213	0.7143	0.7148	0.7347	0.4633	0.4709	0.4898	0.1115
	Ours	0.6845	0.4764	0.7707	0.7571	0.7643	0.5341	0.5319	0.5380	0.0787
SegMaR [27]	Source-Only	0.6468	0.4091	0.6947	0.6943	0.7199	0.4522	0.4648	0.4880	0.1215
	Mean Teacher	0.6597	0.4211	0.7040	0.7147	0.7382	0.4638	0.4783	0.4997	0.1071
	Ours	0.6832	0.4595	0.7298	0.7409	0.7619	0.5012	0.5190	0.5407	0.0787
RISNet [58]	Source-Only	0.6627	0.4543	0.7332	0.7248	0.7310	0.5105	0.5059	0.5085	0.0752
	Mean Teacher	0.7622	0.5962	0.8173	0.8257	0.8400	0.6316	0.6502	0.6650	0.0529
	Ours	0.7627	0.6141	0.8301	0.8338	0.8401	0.6532	0.6621	0.6729	0.0516

learns high quality pseudo labels.

$$\mathcal{D}_{cl} = \{(x_t^{cl}, \hat{y}_t^{cl}) \mid \hat{y}_t^{cl} \geq \tau, \hat{y}_t^{cl} \in y_t^{cl}\}, \quad (10)$$

CLS mechanism guides the model to learn domain invariant features from clean pseudo labels, enhancing the representational power of the target domain and improving the generalization performance of the model. To reduce the domain gap, we introduce an evolving real domain $\hat{\mathcal{D}}_s$ to bridge the source domain \mathcal{D}_s and the target domain \mathcal{D}_t . Specifically, we replace \mathcal{D}_s with $\hat{\mathcal{D}}_s$ to obtain better pseudo labels. Our designs $\hat{\mathcal{D}}_s$ through data fusion, leveraging the clear datasets \mathcal{D}_{cl} from both the source and target domains.

$$\hat{\mathcal{D}}_s = \mathcal{D}_s \cup \mathcal{D}_{cl}. \quad (11)$$

After obtaining $\hat{\mathcal{D}}_s$, a new round of training is initiated using a student-teacher model. The final training objective of our framework can be expressed as follows:

$$\begin{aligned} \min_f \mathbb{E}_{(\hat{x}_s, \hat{y}_s) \sim \hat{\mathcal{D}}_s, x_t \sim \mathcal{D}_t} [\mathcal{L}_{CE}(f(\mathcal{A}(\hat{x}_s)), \hat{y}_s) \\ + \mathcal{L}_{ES}(f(\tilde{\mathcal{A}}(x_t)), fema(\mathcal{A}(x_t)))]. \end{aligned} \quad (12)$$

Through training, the model gradually learns the commonalities and differences between the source and target domain, thereby improving performance on the target domain. This approach not only effectively utilizes labeled source domain data and unlabeled target domain data but also mitigates the domain gap by synthesizing an evolving real domain, providing a novel solution for the unsupervised image segmentation problem.

4 EXPERIMENTS

4.1 Settings

Dataset. To validate the feasibility of the method, we performed evaluations on one SOD dataset and four COD datasets. HKU-IS [38] is a classic SOD benchmark dataset containing 4,447 images with complex backgrounds and multiple salient objects, covering both indoor and outdoor scenes. CAMO [35] consists of 1,250 camouflaged images and 1,250 non-camouflaged images. CHAMELEON [52] includes 76 camouflaged images from natural scenes, focusing

on animal camouflaged cases. COD10K [11] is the largest COD dataset to date, containing 5,056 camouflaged images across five major categories and 69 subcategories. NC4K [44] includes 4,121 real world camouflaged object images.

Task Setup. In this paper, we divide the S2R-COD tasks into $\hat{S}2C$ and $\hat{C}2C$. It is important to note that, regardless of whether the dataset is SOD or COD, the corresponding synthetic COD dataset is used as the source domain. In $\hat{S}2C$ task, we use the synthetic HKU-IS dataset as the source domain, the real unlabeled COD10K training set as the target domain, and evaluate the performance on the COD10K test set. For $\hat{C}2C$ task, we consistently use the real unlabeled COD10K training set as the target domain and conduct final testing on different datasets. Based on the target test set, we adjust the source domain data selection as follows:

Case 1: When the test set is COD10K, the source domain consists of the remaining three synthetic COD datasets.

Case 2: When the test set is CAMO or CHAMELEON, the source domain is composed of the synthetic COD datasets from Case 1 with CAMO or CHAMELEON images removed to prevent target domain data leakage.

Case 3: When the test set is NC4K since removing the corresponding synthetic data for NC4K leaves fewer source domain samples, we additionally introduce synthetic images from the COD10K test set to enhance the diversity of the source domain.

Evaluation Metrics. Referring to previous work [19, 22, 33, 61, 71], we use five metrics to comprehensively evaluate the model performance in COD task, including structure measure (S_α) [7], weighted F-measure (F_β^w) [45], enhanced-alignment measure (E_ϕ) [8, 10], F-measure (F_β) [4], and mean absolute error (M).

Implementation Details. All experiments are conducted on an RTX 3090 GPU and implemented using the PyTorch framework. We adopt SINet [11] as the baseline of COD model and train student model using the Adam optimizer. The training process lasts for 40 epochs with a batch size of 16, initiating with a learning rate of 1e-4 and dividing it by 10 after 30 epochs. In $\hat{S}2C$ task, the smoothing coefficient λ for teacher model is set to 0.996, while the hyperparameters μ and τ of CLS are set to 0.8 and 0.4, respectively.

Table 2: Experimental results on CAMO + NC4K + CHAM. \rightarrow COD10K ($\hat{C}2C$) benchmark.

Model	Setting	$S_\alpha \uparrow$	$F_\beta^w \uparrow$	$E_\phi^{ad} \uparrow$	$E_\phi^{mn} \uparrow$	$E_\phi^{mx} \uparrow$	$F_\beta^{ad} \uparrow$	$F_\beta^{mn} \uparrow$	$F_\beta^{mx} \uparrow$	$M \downarrow$
SINet [11]	Source-Only	0.6606	0.3999	0.6780	0.6807	0.7268	0.4471	0.4694	0.5074	0.1386
	Mean Teacher	0.7299	0.4700	0.7225	0.7544	0.8179	0.5131	0.5607	0.5936	0.0860
	Ours	0.7555	0.5202	0.7730	0.7779	0.8371	0.5679	0.6049	0.6297	0.0650
SINet-v2 [9]	Source-Only	0.6753	0.4499	0.7135	0.7155	0.7519	0.4851	0.5047	0.5431	0.1235
	Mean Teacher	0.6960	0.4958	0.7613	0.7673	0.7818	0.5300	0.5405	0.5624	0.0872
	Ours	0.7211	0.5329	0.8020	0.7975	0.8069	0.5718	0.5817	0.5987	0.0669
SegMaR [27]	Source-Only	0.6670	0.4319	0.6997	0.7033	0.7445	0.4675	0.4843	0.5316	0.1231
	Mean Teacher	0.7037	0.4860	0.7449	0.7574	0.7874	0.5170	0.5388	0.5724	0.0820
	Ours	0.7312	0.5369	0.7959	0.7903	0.8065	0.5755	0.5894	0.6109	0.0660
RISNet [58]	Source-Only	0.7192	0.5472	0.8054	0.7959	0.8015	0.5859	0.5875	0.6018	0.0702
	Mean Teacher	0.7640	0.6006	0.8096	0.8108	0.8494	0.6088	0.6339	0.6844	0.0629
	Ours	0.7797	0.6373	0.8263	0.8350	0.8603	0.6539	0.6647	0.6958	0.0507

Table 3: Experimental results on three additional $\hat{C}2C$ benchmarks, including (CAMO + NC4K \rightarrow CHAM.), (CHAM. + NC4K \rightarrow CAMO), and (CAMO + CHAM. + COD10K \rightarrow NC4K).

Test Dataset	Setting	$S_\alpha \uparrow$	$F_\beta^w \uparrow$	$E_\phi^{ad} \uparrow$	$E_\phi^{mn} \uparrow$	$E_\phi^{mx} \uparrow$	$F_\beta^{ad} \uparrow$	$F_\beta^{mn} \uparrow$	$F_\beta^{mx} \uparrow$	$M \downarrow$
CHAMELEON [52]	Source-Only	0.7063	0.5076	0.7939	0.7319	0.7773	0.5997	0.5711	0.6017	0.1189
	Mean Teacher	0.7667	0.5776	0.8287	0.7907	0.8360	0.6572	0.6489	0.6912	0.0927
	Ours	0.7801	0.6049	0.8558	0.8240	0.8731	0.6824	0.6707	0.7090	0.0715
CAMO [35]	Source-Only	0.6387	0.4458	0.7139	0.6361	0.6643	0.5505	0.5138	0.5411	0.2002
	Mean Teacher	0.7055	0.5163	0.7872	0.7064	0.7545	0.6388	0.5896	0.6281	0.1414
	Ours	0.7158	0.5303	0.7994	0.7113	0.7781	0.6570	0.6021	0.6508	0.1301
NC4K [44]	Source-Only	0.7554	0.5849	0.8128	0.7791	0.8224	0.6619	0.6541	0.6863	0.0926
	Mean Teacher	0.7887	0.5890	0.8271	0.7921	0.8594	0.6889	0.6848	0.7411	0.0880
	Ours	0.7946	0.6359	0.8528	0.7967	0.8698	0.7297	0.7076	0.7560	0.0737

In contrast, for $\hat{C}2C$ task, these values are adjusted to 0.9996, 1.0, and 0.5, respectively. The number of cycling iterations is set to 2. During evaluation, only the teacher model is reserved for inference.

4.2 Results and Analysis

Comparison with Baselines. In Tab. 1 and Tab. 2, we compare the Source-Only baseline, Mean Teacher [56], and our method on $\hat{S}2C$ and $\hat{C}2C$ tasks. From the experimental results, we observe that Source-Only exhibits limited performance across all models, indicating a significant domain gap between synthetic and real images. Mean Teacher improves model performance to some extent by introducing target domain data. However, since this method does not filter the pseudo labels generated by the teacher model, a performance drop is observed on certain metrics for some models. For example, in $\hat{S}2C$ task, both SINet [11] and SINet-v2 [9] under the Mean Teacher method show a certain decrease in MAE and E_ϕ^{ad} compared to the Source-Only baseline, with the E_ϕ^{ad} metric averaging a 2% drop. This suggests that unfiltered pseudo labels may introduce noise, which negatively impacts the model performance. Our proposed method outperforms both Source-Only and Mean Teacher on all metrics in $\hat{S}2C$ and $\hat{C}2C$ tasks. For example, on SINet, F_β^w increased by 11.1% and 12%, and F_β^{mx} increased by 12.5% and 13.5%. Compared to Mean Teacher, F_β^w and F_β^{mx} also increased by

6.4%, 5%, and 3.6%, 4.4% respectively. By comparing the overall experimental data in Tab. 1 and Tab. 2, it can be observed that the performance on $\hat{S}2C$ task is significantly lower than that on $\hat{C}2C$ tasks across different models. This result indicates that, despite using synthetic COD datasets as the source domain, there is still a significant domain gap between SOD and COD. However, it is worth noting that despite this domain gap, synthesizing a large amount of COD data from easily accessible SOD images remains a valuable research direction. Synthetic data provides an initial training basis for the model, especially in scenarios where the cost of labeling real COD data is high [5, 39, 54, 76, 78], and can effectively alleviate the problem of data scarcity. As documented in Tab. 3, we conduct comprehensive evaluations on three mainstream COD datasets using SINet as the base model, validating the effectiveness of our proposed method. Compared with Source-Only and Mean Teacher, the proposed method presents a substantial advantage in terms of key performance indicators.

Comparison with Other Related Methods. According to the experimental results on the COD10K benchmark for S2R-COD in Tab. 4, our method significantly outperforms existing UDA approaches across multiple critical metrics. Specifically, our approach achieves 0.7555 in comprehensive performance metric S_α and 0.5202 in F_β^w , surpassing the suboptimal Mean Teacher [56] method by

Table 4: Comparison of different UDA methods on CAMO + NC4K + CHAM. → COD10K ($\hat{C}2C$) benchmark.

Method	$S_\alpha \uparrow$	$F_\beta^w \uparrow$	$E_\phi^{ad} \uparrow$	$E_\phi^{mn} \uparrow$	$E_\phi^{mx} \uparrow$	$F_\beta^{ad} \uparrow$	$F_\beta^{mn} \uparrow$	$F_\beta^{mx} \uparrow$	$M \downarrow$
Source-Only	0.6606	0.3999	0.6780	0.6807	0.7268	0.4471	0.4694	0.5074	0.1386
FDA [62]	0.6847	0.4186	0.6896	0.7089	0.7618	0.4627	0.4885	0.5298	0.1064
DANN [14]	0.7050	0.4572	0.7180	0.7382	0.7831	0.4939	0.5232	0.5571	0.0906
Mean Teacher [56]	0.7299	0.4700	0.7225	0.7544	0.8179	0.5131	0.5607	0.6174	0.0873
PMT [2]	0.6737	0.4861	0.7442	0.7423	0.7442	0.5227	0.5189	0.5205	0.0797
Ours	0.7555	0.5202	0.7730	0.7779	0.8371	0.5679	0.6049	0.6530	0.0650

Table 5: The ablation study of ES Loss and Confident Label Selection (CLS). MT denotes the Mean Teacher method.

HKU-IS → COD10K ($\hat{S}2C$)						
Model	Setting	$S_\alpha \uparrow$	$F_\beta^w \uparrow$	$E_\phi^{mn} \uparrow$	$F_\beta^{mn} \uparrow$	$M \downarrow$
SINet [11]	MT+ \mathcal{L}_{CE}	0.6984	0.4165	0.7177	0.5106	0.0915
	MT+ \mathcal{L}_{ES}	0.7020	0.4531	0.7362	0.5284	0.0900
	MT+ \mathcal{L}_{ES} +CLS	0.7136	0.4814	0.7433	0.5572	0.0717
SINet-v2 [9]	MT+ \mathcal{L}_{CE}	0.6485	0.4213	0.7148	0.4709	0.1115
	MT+ \mathcal{L}_{ES}	0.6624	0.4426	0.7379	0.4928	0.0974
	MT+ \mathcal{L}_{ES} +CLS	0.6845	0.4764	0.7571	0.5319	0.0787
CAMO + NC4K + CHAM. → COD10K ($\hat{C}2C$)						
Model	Setting	$S_\alpha \uparrow$	$F_\beta^w \uparrow$	$E_\phi^{mn} \uparrow$	$F_\beta^{mn} \uparrow$	$M \downarrow$
SINet [11]	MT+ \mathcal{L}_{CE}	0.7299	0.4700	0.7544	0.5607	0.0873
	MT+ \mathcal{L}_{ES}	0.7332	0.4812	0.7602	0.5658	0.0853
	MT+ \mathcal{L}_{ES} +CLS	0.7555	0.5202	0.7779	0.6049	0.0650
SINet-v2 [9]	MT+ \mathcal{L}_{CE}	0.6960	0.4958	0.7673	0.5405	0.0872
	MT+ \mathcal{L}_{ES}	0.7032	0.5015	0.7709	0.5475	0.0845
	MT+ \mathcal{L}_{ES} +CLS	0.7211	0.5329	0.7975	0.5817	0.0669

2.5% and 5.0%, respectively. Compared to classical methods FDA [62] and DANN [1], our method demonstrates even greater improvements of 7.0% and 5.0% in S_α . The robust performance on fine grained metrics, such as E_ϕ^{mx} (0.8371) and F_β^{mx} (0.6530), highlights the model effectiveness in handling extreme target domain samples. Additionally, MAE (0.0650) indicates a 28.3% reduction in false detection rates compared to DANN [1], further validating our method superiority in domain adaptation.

4.3 Ablation Studies

Effect of ES Loss and CLS. The two key innovations in our work are ES loss and CLS. The ES Loss is specifically designed to enhance model robustness by improving its ability to handle camouflaged object boundaries and high confidence regions, thereby facilitating better adaptation to challenging target domains. Meanwhile, the CLS mechanism is introduced to refine the pseudo labels generated by the model, ensuring that cleaner and more reliable labels are retained in the source domain. This, in turn, mitigates the negative impact of noisy pseudo labels and helps to reduce the domain gap.

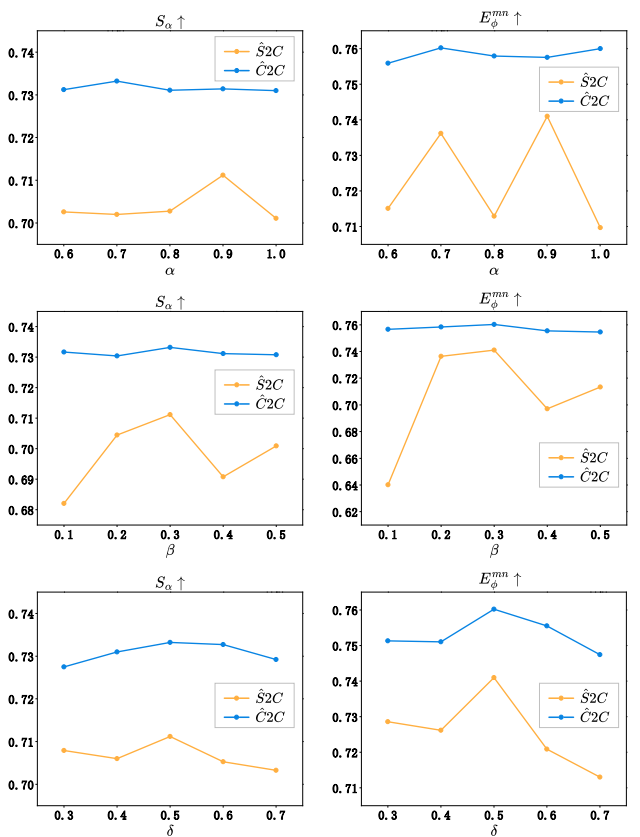


Figure 4: The impact of different hyperparameter combinations α , β , δ on ES Loss under the HKU-IS → COD10K ($\hat{S}2C$) and CAMO + NC4K + CHAM. → COD10K ($\hat{C}2C$) benchmarks. The left figure presents the model performance in terms of S_α , while the right figure shows the results for E_ϕ^{mn} .

To systematically evaluate the effectiveness of these two components, we conduct an ablation study and present the results in Tab. 5. The comparison across different model settings demonstrates that both the ES Loss and CLS contribute positively to performance improvements in both $\hat{S}2C$ task, whereas the CLS brings greater improvements in $\hat{C}2C$ tasks. We hypothesize that in scenarios with a large domain gap ($\hat{S}2C$), edge alignment and salient

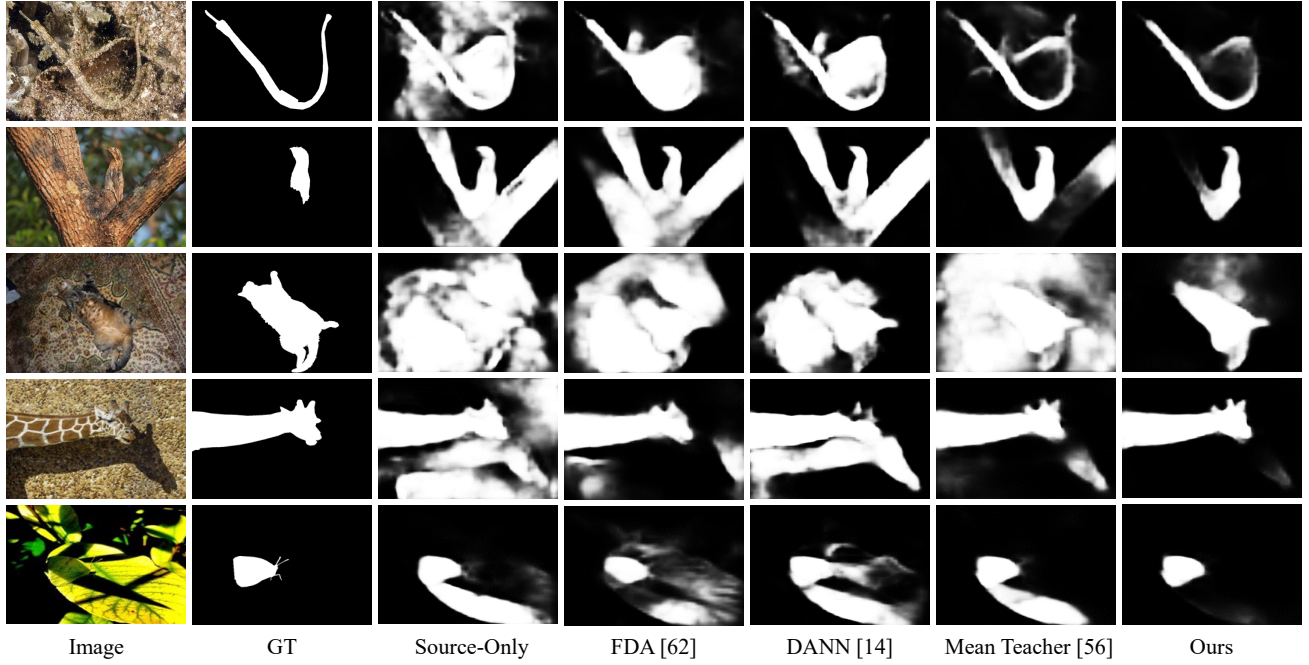


Figure 5: Visual comparisons with UDA methods on different types of samples. Please zoom in for details.

region weighting effectively enhance the model ability to capture target domain features. In contrast, for $\hat{C}2C$ tasks where the domain gap is smaller, the quality of pseudo labels plays a more critical role in determining model performance.

Evaluation of Hyperparameters. In Fig. 4, we conduct a detailed analysis of the impact of hyperparameters α , β and δ in the ES Loss on the COD10K benchmark. Specifically, we examine how variations in these parameters influence the model performance in terms of S_α and E_ϕ^{mn} . From the experimental results, we notably observe that for $\hat{S}2C$ task achieves its best performance when configured with $\alpha = 0.9$, $\beta = 0.3$, and $\delta = 0.5$, which corresponds to the edge loss, weighted cross-entropy loss, and weight matrix, respectively. In contrast, for $\hat{C}2C$ task, the optimal choice of α differs, with $\alpha = 0.7$ achieving better performance, while the other two parameters remain the same as in $\hat{S}2C$ task.

4.4 Qualitative Evaluation

Visualization Analysis. In Fig. 5, we present the visualization results of the SINet [11] on the COD10K dataset using different UDA methods. The Source-Only (Column 2) exhibits significant missegmentation due to domain differences, such as misidentifying branch textures as camouflaged objects. While the Mean Teacher [56] method (Column 6) improves overall detection, it suffers from significant edge blurring. Other UDA methods also tend to mistakenly segment regions with similar characteristics around the target, a problem particularly evident in the fourth and fifth images, where shadows corresponding to camouflaged objects are frequently misidentified as part of the target. In contrast, our method (Column 7) effectively mitigates these issues by leveraging edge alignment constrained by ES Loss to achieve precise target contour

localization in complex backgrounds (e.g., the butterfly in Row 5). Additionally, the CLS mechanism effectively suppresses artifactual noise (as seen in the background region of Row 4) while reducing the missegmentation of similar regions around the target. These improvements significantly enhance detection accuracy, further demonstrating the superior performance of our approach.

5 Conclusion

This paper introduces a novel COD task, termed S2R-COD, which aims to leverage a set of easily accessible, annotated synthetic images to enhance model performance on real unlabeled target domain images. To achieve this, we propose CSRDA, a framework that employs a cycling student-teacher model to generate pseudo labels for real target domain images. Using CLS to filter these pseudo labels and introduce an evolving real domain to bridge the gap between the labeled source domain and the unlabeled target domain, thereby reducing domain discrepancies. Notably, we propose an innovative ES loss function to improve the model ability to capture target domain features. Furthermore, we establish a set of strong baselines to highlight the effectiveness of our approach. In summary, we hope this study provides new insights into synthetic-to-real camouflaged object detection.

Acknowledgments

This work was supported by the National Natural Science Foundation of China (Grant No. 62406071, Grant No. 62495061), and the China Postdoctoral Science Foundation (Grant No. 2025T180422, Grant No. 2024M761682, Grant No. GZB20240357) and Shui Mu Tsinghua Scholar (Grant No. 2024SM079).

References

- [1] Hana Ajakan, Pascal Germain, Hugo Larochelle, François Laviolette, and Mario Marchand. 2014. Domain-adversarial neural networks. *arXiv preprint arXiv:1412.4446* (2014).
- [2] Atif Belal, Akhil Meethal, Francisco Perdigon Romero, Marco Pedersoli, and Eric Granger. 2024. Multi-source domain adaptation for object detection with prototype-based mean teacher. In *WACV*.
- [3] Shai Ben-David, John Blitzer, Koby Crammer, and Fernando Pereira. 2006. Analysis of representations for domain adaptation. *NeurIPS* (2006).
- [4] Ali Borji, Ming-Ming Cheng, Huaiju Jiang, and Jia Li. 2015. Salient object detection: A benchmark. *IEEE TIP* (2015).
- [5] Zhenhan Chen, Xuying Zhang, Tian-Zhu Xiang, and Ying Tai. 2024. Adaptive guidance learning for camouflaged object detection. *arXiv preprint arXiv:2405.02824* (2024).
- [6] Shupeng Cheng, Ge-Peng Ji, Pengda Qin, Deng-Ping Fan, Bowen Zhou, and Peng Xu. 2023. Large model based referring camouflaged object detection. *arXiv preprint arXiv:2311.17122* (2023).
- [7] Deng-Ping Fan, Ming-Ming Cheng, Yun Liu, Tao Li, and Ali Borji. 2017. Structure-measure: A new way to evaluate foreground maps. In *ICCV*.
- [8] Deng-Ping Fan, Cheng Gong, Yang Cao, Bo Ren, Ming-Ming Cheng, and Ali Borji. 2018. Enhanced-alignment measure for binary foreground map evaluation. *arXiv preprint arXiv:1805.10421* (2018).
- [9] Deng-Ping Fan, Ge-Peng Ji, Ming-Ming Cheng, and Ling Shao. 2021. Concealed object detection. *IEEE TPAMI* (2021).
- [10] Deng-Ping Fan, Ge-Peng Ji, Xuebin Qin, and Ming-Ming Cheng. 2021. Cognitive vision inspired object segmentation metric and loss function. *Scientia Sinica Informationis* (2021).
- [11] Deng-Ping Fan, Ge-Peng Ji, Guolei Sun, Ming-Ming Cheng, Jianbing Shen, and Ling Shao. 2020. Camouflaged object detection. In *CVPR*.
- [12] Galun, Sharon, Basri, and Brandt. 2003. Texture segmentation by multiscale aggregation of filter responses and shape elements. In *ICCV*.
- [13] Yaroslav Ganin and Victor Lempitsky. 2015. Unsupervised domain adaptation by backpropagation. In *ICML*.
- [14] Yaroslav Ganin, Evgeniya Ustinova, Hana Ajakan, Pascal Germain, Hugo Larochelle, François Laviolette, Mario March, and Victor Lempitsky. 2016. Domain-adversarial training of neural networks. *MLR* (2016).
- [15] Arthur Gretton, Karsten Borgwardt, Malte Rasch, Bernhard Schölkopf, and Alex Smola. 2006. A kernel method for the two-sample-problem. *NeurIPS* (2006).
- [16] Arthur Gretton, Karsten M Borgwardt, Malte J Rasch, Bernhard Schölkopf, and Alexander Smola. 2012. A kernel two-sample test. *MLR* (2012).
- [17] Jean-Bastien Grill, Florian Strub, Florent Altché, Corentin Tallec, Pierre Richemond, Elena Buchatskaya, Carl Doersch, Bernardo Avila Pires, Zhaohan Guo, Mohammad Ghehsaghli Azar, et al. 2020. Bootstrap your own latent-a new approach to self-supervised learning. *NeurIPS* (2020).
- [18] Chao Hao, Zitong Yu, Xin Liu, Jun Xu, Huanjing Yue, and Jingyu Yang. 2025. A simple yet effective network based on vision transformer for camouflaged object and salient object detection. *IEEE TIP* (2025).
- [19] Chunning He, Kai Li, Yachao Zhang, Longxiang Tang, Yulun Zhang, Zhenhua Guo, and Xiu Li. 2023. Camouflaged object detection with feature decomposition and edge reconstruction. In *CVPR*.
- [20] Chunning He, Kai Li, Yachao Zhang, Guoxia Xu, Longxiang Tang, Yulun Zhang, Zhenhua Guo, and Xiu Li. 2023. Weakly-supervised concealed object segmentation with sam-based pseudo labeling and multi-scale feature grouping. *NIPS* (2023).
- [21] Jianqin Yin Yanbin Han Wendi Hou and Jinping Li. 2011. Detection of the mobile object with camouflage color under dynamic background based on optical flow. *Procedia Eng* (2011).
- [22] Jian Hu, Jiayi Lin, Shaogang Gong, and Weitong Cai. 2024. Relax image-specific prompt requirement in sam: A single generic prompt for segmenting camouflaged objects. In *AAAI*.
- [23] Xiaobin Hu, Shuo Wang, Xuebin Qin, Hang Dai, Wenqi Ren, Donghao Luo, Ying Tai, and Ling Shao. 2023. High-resolution iterative feedback network for camouflaged object detection. In *AAAI*.
- [24] Zhou Huang, Hang Dai, Tian-Zhu Xiang, Shuo Wang, Huai-Xin Chen, Jie Qin, and Huan Xiong. 2023. Feature shrinkage pyramid for camouflaged object detection with transformers. In *CVPR*.
- [25] Ge-Peng Ji, Deng-Ping Fan, Yu-Cheng Chou, Dengxin Dai, Alexander Liniger, and Luc Van Gool. 2023. Deep gradient learning for efficient camouflaged object detection. *MIR* (2023).
- [26] Ge-Peng Ji, Lei Zhu, Mingchen Zhuge, and Keren Fu. 2022. Fast camouflaged object detection via edge-based reversible re-calibration network. *PR* (2022).
- [27] Qi Jia, Shuilian Yao, Yu Liu, Xin Fan, Risheng Liu, and Zhongxuan Luo. 2022. Segment, magnify and reiterate: Detecting camouflaged objects the hard way. In *CVPR*.
- [28] Lu Jiang, Zhengyuan Zhou, Thomas Leung, Li-Jia Li, and Li Fei-Fei. 2018. Mentor-net: Learning data-driven curriculum for very deep neural networks on corrupted labels. In *ICML*.
- [29] Nobukatsu Kajiura, Hong Liu, and Shin-ichi Satoh. 2021. Improving camouflaged object detection with the uncertainty of pseudo-edge labels. In *ACM MM*.
- [30] Guoliang Kang, Lu Jiang, Yi Yang, and Alexander G Hauptmann. 2019. Contrastive adaptation network for unsupervised domain adaptation. In *CVPR*.
- [31] Abbas Khan, Mustaqeem Khan, Wail Gueaieb, Abdulmotaleb El Saddik, Giulia De Masi, and Fakhri Karray. 2024. CamoFocus: Enhancing camouflage object detection with split-feature focal modulation and context refinement. In *WACV*.
- [32] Taeksoo Kim, Moonsu Cha, Hyunsoo Kim, Jung Kwon Lee, and Jiwon Kim. 2017. Learning to discover cross-domain relations with generative adversarial networks. In *ICML*.
- [33] Xunfa Lai, Zhiyu Yang, Jie Hu, Shengchuan Zhang, Liujuan Cao, Guannan Jiang, Zhiyu Wang, Songan Zhang, and Rongrong Ji. 2024. CamoTeacher: Dual-Rotation Consistency Learning for Semi-Supervised Camouflaged Object Detection. In *ECCV*.
- [34] Zhengfeng Lai, Haoping Bai, Haotian Zhang, Xianzhi Du, Jiulong Shan, Yinfei Yang, Chen-Nee Chuah, and Meng Cao. 2024. Empowering unsupervised domain adaptation with large-scale pre-trained vision-language models. In *WACV*.
- [35] Trung-Nghia Le, Tam V Nguyen, Zhongliang Nie, Minh-Triet Tran, and Akihiro Sugimoto. 2019. Anabanch network for camouflaged object segmentation. *CVIU* (2019).
- [36] Dong-Hyun Lee et al. 2013. Pseudo-label: The simple and efficient semi-supervised learning method for deep neural networks. In *Workshop on Challenges in Representation Learning*.
- [37] Aixuan Li, Jing Zhang, Yunqiu Lv, Bowen Liu, Tong Zhang, and Yuchao Dai. 2021. Uncertainty-aware joint salient object and camouflaged object detection. In *CVPR*.
- [38] Guanbin Li and Yizhou Yu. 2015. Visual saliency based on multiscale deep features. In *CVPR*.
- [39] Peng Li, Xuefeng Yan, Hongwei Zhu, Mingqiang Wei, Xiao-Ping Zhang, and Jing Qin. 2022. Findnet: Can you find me? boundary-and-texture enhancement network for camouflaged object detection. *IEEE TIP* (2022).
- [40] Xiaofei Li, Jiaxin Yang, Shuhao Li, Jun Lei, Jun Zhang, and Dong Chen. 2023. Locate, Refine and Restore: A Progressive Enhancement Network for Camouflaged Object Detection.. In *IJCAI*.
- [41] Yi Liu, Dingwen Zhang, Qiang Zhang, and Jungong Han. 2021. Integrating part-object relationship and contrast for camouflaged object detection. *IEEE TIFS* (2021).
- [42] Ziyang Luo, Nian Liu, Wangbo Zhao, Xuguang Yang, Dingwen Zhang, Deng-Ping Fan, Fahad Khan, and Junwei Han. 2024. Vscode: General visual salient and camouflaged object detection with 2d prompt learning. In *CVPR*.
- [43] Yunqiu Lv, Jing Zhang, Yuchao Dai, Aixuan Li, Nick Barnes, and Deng-Ping Fan. 2023. Toward deeper understanding of camouflaged object detection. *IEEE TCSV* (2023).
- [44] Yunqiu Lv, Jing Zhang, Yuchao Dai, Aixuan Li, Bowen Liu, Nick Barnes, and Deng-Ping Fan. 2021. Simultaneously localize, segment and rank the camouflaged objects. In *CVPR*.
- [45] Ran Margolin, Lili Zelnik-Manor, and Ayallet Tal. 2014. How to evaluate foreground maps?. In *CVPR*.
- [46] Haiyang Mei, Ge-Peng Ji, Ziqi Wei, Xin Yang, Xiaopeng Wei, and Deng-Ping Fan. 2021. Camouflaged object segmentation with distraction mining. In *CVPR*.
- [47] Thanh-Danh Nguyen, Anh-Khoa Nguyen Vu, Nhat-Duy Nguyen, Vinh-Tiep Nguyen, Thanh Duc Ngo, Thanh-Toan Do, Minh-Triet Tran, and Tam V Nguyen. 2024. The Art of Camouflage: Few-Shot Learning for Animal Detection and Segmentation. *IEEE Access* (2024).
- [48] Yuxin Pan, Yiwang Chen, Qiang Fu, Ping Zhang, Xin Xu, et al. 2011. Study on the camouflaged target detection method based on 3D convexity. *MAS* (2011).
- [49] Youwei Pang, Xiaoqi Zhao, Tian-Zhu Xiang, Lihe Zhang, and Huchuan Lu. 2022. Zoom in and out: A mixed-scale triplet network for camouflaged object detection. In *CVPR*.
- [50] Chennamsetty Pulla Rao, A Guruva Reddy, and CB Rama Rao. 2020. Camouflaged object detection for machine vision applications. (2020).
- [51] Jian Shen, Yanru Qu, Weinan Zhang, and Yong Yu. 2018. Wasserstein distance guided representation learning for domain adaptation. In *AAAI*.
- [52] Przemyslaw Skurowski, Hassan Abdulameer, Jakub Blaszczyk, Tomasz Depta, Adam Kornacki, and Przemyslaw Koziel. 2018. Animal camouflage analysis: Chameleon database. *Unpublished Manuscript* (2018).
- [53] Yujia Sun, Geng Chen, Tao Zhou, Yi Zhang, and Nian Liu. 2021. Context-aware cross-level fusion network for camouflaged object detection. *arXiv preprint arXiv:2105.12555* (2021).
- [54] Yujia Sun, Shuo Wang, Chenglizhao Chen, and Tian-Zhu Xiang. 2022. Boundary-guided camouflaged object detection. *arXiv preprint arXiv:2207.00794* (2022).
- [55] Ariel Tankus and Yechezkel Yeshurun. 1998. Detection of regions of interest and camouflage breaking by direct convexity estimation. In *Proceedings 1998 IEEE Workshop on Visual Surveillance*.
- [56] Antti Tarvainen and Harri Valpola. 2017. Mean teachers are better role models: Weight-averaged consistency targets improve semi-supervised deep learning results. *NeurIPS* (2017).

[57] Eric Tzeng, Judy Hoffman, Kate Saenko, and Trevor Darrell. 2017. Adversarial discriminative domain adaptation. In *CVPR*. 7167–7176.

[58] Liqiong Wang, Jinyu Yang, Yanfu Zhang, Fangyi Wang, and Feng Zheng. 2024. Depth-Aware Concealed Crop Detection in Dense Agricultural Scenes. In *CVPR*.

[59] Yinghui Xing, Dexuan Kong, Shizhou Zhang, Geng Chen, Lingyan Ran, Peng Wang, and Yanning Zhang. 2023. Pre-train, adapt and detect: Multi-task adapter tuning for camouflaged object detection. *arXiv preprint arXiv:2307.10685* (2023).

[60] Jinnan Yan, Trung-Nghia Le, Khanh-Duy Nguyen, Minh-Triet Tran, Thanh-Toan Do, and Tam V Nguyen. 2021. Mirrornet: Bio-inspired camouflaged object segmentation. *IEEE Access* (2021).

[61] Fan Yang, Qiang Zhai, Xin Li, Rui Huang, Ao Luo, Hong Cheng, and Deng-Ping Fan. 2021. Uncertainty-guided transformer reasoning for camouflaged object detection. In *ICCV*.

[62] Yanchao Yang and Stefano Soatto. 2020. Fda: Fourier domain adaptation for semantic segmentation. In *CVPR*.

[63] Yang Yang and Qiang Zhang. 2023. Finding camouflaged objects along the camouflage mechanisms. *IEEE TCSV* (2023).

[64] Zili Yi, Hao Zhang, Ping Tan, and Minglun Gong. 2017. Dualgan: Unsupervised dual learning for image-to-image translation. In *ICCV*.

[65] Guanghui Yue, Houlu Xiao, Hai Xie, Tianwei Zhou, Wei Zhou, Weiqing Yan, Baoquan Zhao, Tianfu Wang, and Qiuiping Jiang. 2023. Dual-constraint coarse-to-fine network for camouflaged object detection. *IEEE TCSV* (2023).

[66] Qiang Zhai, Xin Li, Fan Yang, Chenglizhao Chen, Hong Cheng, and Deng-Ping Fan. 2021. Mutual graph learning for camouflaged object detection. In *CVPR*.

[67] Qiang Zhai, Xin Li, Fan Yang, Zhicheng Jiao, Ping Luo, Hong Cheng, and Zicheng Liu. 2022. MGL: Mutual graph learning for camouflaged object detection. *IEEE TIP* (2022).

[68] Cong Zhang, Hongbo Bi, Tian-Zhu Xiang, Ranwan Wu, Jinghui Tong, and Xiufang Wang. 2023. Collaborative camouflaged object detection: A large-scale dataset and benchmark. *IEEE TNNLS* (2023).

[69] Qiao Zhang, Xiaoxiao Sun, Yurui Chen, Yanliang Ge, and Hongbo Bi. 2023. Attention-induced semantic and boundary interaction network for camouflaged object detection. *CVIU* (2023).

[70] Xuying Zhang, Bowen Yin, Zheng Lin, Qibin Hou, Deng-Ping Fan, and Ming-Ming Cheng. 2025. Referring camouflaged object detection. *IEEE TPAMI* (2025).

[71] Yi Zhang and Chengyi Wu. 2023. Unsupervised camouflaged object segmentation as domain adaptation. In *ICCVW*.

[72] Pancheng Zhao, Peng Xu, Pengda Qin, Deng-Ping Fan, Zhicheng Zhang, Guoli Jia, Bowen Zhou, and Jufeng Yang. 2024. Lake-red: Camouflaged images generation by latent background knowledge retrieval-augmented diffusion. In *CVPR*.

[73] Dehua Zheng, Xiaochen Zheng, Laurence T Yang, Yuan Gao, Chenlu Zhu, and Yiheng Ruan. 2023. Mffn: Multi-view feature fusion network for camouflaged object detection. In *WACV*.

[74] Yijie Zhong, Bo Li, Lv Tang, Senyun Kuang, Shuang Wu, and Shouhong Ding. 2022. Detecting camouflaged object in frequency domain. In *CVPR*.

[75] Tao Zhou, Yi Zhou, Chen Gong, Jian Yang, and Yu Zhang. 2022. Feature aggregation and propagation network for camouflaged object detection. *IEEE TIP* (2022).

[76] Hongwei Zhu, Peng Li, Haoran Xie, Xuefeng Yan, Dong Liang, Dapeng Chen, Mingqiang Wei, and Jing Qin. 2022. I can find you! boundary-guided separated attention network for camouflaged object detection. In *AAAI*.

[77] Jun-Yan Zhu, Taesung Park, Phillip Isola, and Alexei A Efros. 2017. Unpaired image-to-image translation using cycle-consistent adversarial networks. In *ICCV*.

[78] Mingchen Zhuge, Xiankai Lu, Yiyou Guo, Zhihua Cai, and Shuhan Chen. 2022. CubeNet: X-shape connection for camouflaged object detection. *PR* (2022).